Micelles

DOI: 10.1002/anie.201003066

Pointed-Oval-Shaped Micelles from Crystalline-Coil Block Copolymers by Crystallization-Driven Living Self-Assembly**

Alejandro Presa Soto, Joe B. Gilroy, Mitchell A. Winnik, and Ian Manners**

Self-assembly of block copolymers in block-selective solvents can lead to a variety of different morphologies with shape- and composition-dependent potential applications in areas as diverse as drug delivery and nanolithography.[1] Amorphous block copolymers usually give rise to spherical micelles in selective solvents, but since the mid 1990s various strategies[2] that promote the formation of other morphologies including cylinders[3,4] or cylinder networks,[5] disks,[6] helices,[7] Janus micelles,[8] toroids,[9] nanotubes,[10] and other complex forms[11–13] have been developed.

Previous work on the solution self-assembly of diblock copolymers has shown that the presence of crystalline core-forming blocks such as poly(ferrocenyldimethylsilane) (PFS), polyethylene, polyacrylonitrile, polycaprolactone, and poly(ethylene oxide) promote the formation of morphologies with low interfacial curvature such as cylinders and platelets.[4,14] Moreover, recent studies of PFS block copolymers have revealed that on addition of further unimer, epitaxial growth from the exposed crystalline cores of the ends of cylindrical micelles or the edges of platelets is possible to generate hierarchical micelle architectures such as block co-micelles and scarf structures, respectively.[15] This crystallization-driven living self-assembly process has enabled the preparation of well-defined self-assembled structures with spatially defined attachment of nanoparticles and oxide surface coatings.[16] Here we report that by using this crystallization-driven living self-assembly approach, the formation of unusual nanoscopic architectures such as pointed ovals and hierarchical pointed-oval-based co-micelle architectures is also possible.

We used two types of asymmetric, narrow polydispersity crystalline-coil, PFS core-forming diblock copolymers: firstly, PFS_{34}–$P2VP_{272}$ (P2VP = poly(2-vinylpyridine))[17,19] to generate cylindrical micelles, especially short "seed" micelles, and, second, PFS_{54}–PP_{290}[18,19] (PP = poly[bis(trifluoroethoxy)-phosphazene]; Scheme 1 and Supporting Information Table S1).

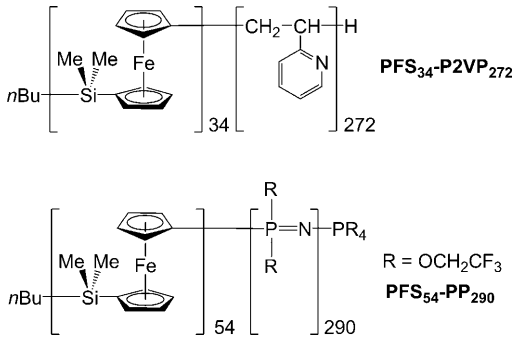

Scheme 1. Structures of PFS_{34}–$P2VP_{272}$ and PFS_{54}–PP_{290}. The numbers in subscript refer to the number-average degree of polymerization (DP_n).

Previous studies have shown that PFS–P2VP block copolymers such as PFS_{34}–$P2VP_{272}$ with a long P2VP segment self-assemble to form cylinders with a crystalline PFS core and a P2VP corona in 2-propanol (*i*PrOH), a selective solvent for the P2VP block.[17] To explore the use of PFS_{54}–PP_{290} in crystallization-driven living self-assembly,[20] seed micelles of PFS_{34}–$P2VP_{272}$ were used as initiators. The seed micelles were generated by sonication of long cylindrical micelles (length 3 to 10 μm (by TEM, see Figure S2) and height 8 to 12 nm (by AFM, see Figure S3)). In our first set of exploratory experiments, a solution of the cylinders (0.0625 mg mL^{-1}) was subjected to sonication for 5 min. This led to shortened PFS_{34}–$P2VP_{272}$ seeds that were polydisperse in length (number average length $L_n = 215$ nm (by TEM), $L_w/L_n = 1.63$ (Figures 1a, S4a, S5a, and S7), and uniform in height (ca. 10 nm by AFM; Figure S6)). We took four aliquots of different volumes of the seed solution and added *i*PrOH to a constant volume of 4 mL (Table S3). To these solutions we then added 0.2 mL of a 10 mg mL^{-1} solution of unimers of the diblock copolymer PFS_{54}–PP_{290} in THF, a good solvent for both blocks. The solution was shaken manually for 10 s and then the micelle growth was monitored using dynamic light scattering (DLS) until the apparent hydrodynamic radius ($R_{h,app}$) of the micelles reached a constant value after 24 h (see Figure S8 and Table S4). Unexpectedly, in contrast to the results of previous studies which led to linear cylindrical triblock co-micelles through epitaxial growth of the PFS core from added block copolymer from the exposed ends of the seeds,[15] TEM analysis revealed the presence of pointed-oval-

[*] Dr. A. Presa Soto, Dr. J. B. Gilroy, Prof. I. Manners
School of Chemistry, University of Bristol
Cantock's Close, Bristol, BS8 1TS (UK)
E-mail: ian.manners@bristol.ac.uk
Prof. M. A. Winnik
Department of Chemistry, University of Toronto
80 St. George Street, Toronto, Ontario M5S 3H6 (Canada)
E-mail: m.winnik@chem.utoronto.ca

[**] A.P.S. is grateful to the EU for a Marie Curie postdoctoral fellowship. J.B.G. is grateful to the NSERC of Canada for a postdoctoral fellowship. We are grateful to Dr. Torben Gädt for the preparation of the block copolymer PFS_{34}–$P2VP_{272}$. I.M. thanks the EU for a Marie Curie Chair, a Reintegration grant, and an Advanced Investigator Grant, and the Royal Society for a Wolfson Research Merit Award. M.A.W. also thanks the NSERC for financial support.

Supporting information for this article is available on the WWW under http://dx.doi.org/10.1002/anie.201003066.

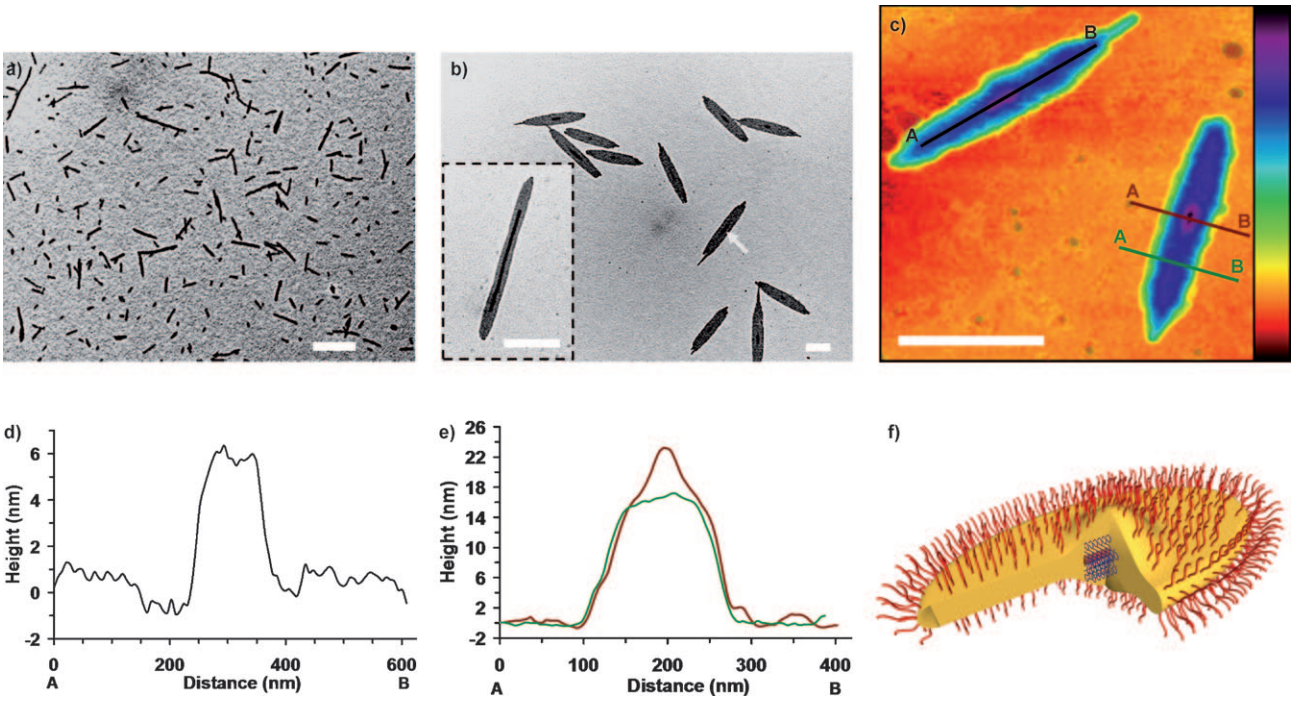

Figure 1. a) Bright field TEM image of the PFS_{34}–$P2VP_{272}$ micelle seeds. b) Bright field TEM image of the pointed-oval-shaped micelles obtained using the conditions described in entries 2 and 3 (inset image) of Table S3. The white arrow shows the seed of PFS_{34}–$P2VP_{272}$. c) AFM height image of the micelles prepared using the conditions described in entry 4 of Table S3. d,e) Cross-sectional height profiles along the long axis of the oval crossing the central cylinder seed (d) and across the micelle (e) crossing the cylinder seed (dark red) and the body of the micelle (green). f) Idealized graphic representation of the pointed-oval-shaped micelle. The PFS core is represented in orange (central cylinder of PFS–P2VP) and yellow (body of the oval of PFS–PP) and the coronas in red (PP) and blue (P2VP). Scale bars correspond to 500 nm.

shaped micelles where PFS_{54}–PP_{290} had grown selectively from the small cylindrical seeds of PFS_{34}–$P2VP_{272}$ (Figure 1b).

The shape and size of the resulting micelles were found to depend on the length of the central cylinder seed and the relative amount of seeds and unimers in the different experiments. The larger PFS_{34}–$P2VP_{272}$ seeds led to the formation of more rectangular shapes (for the case of a very large seed see inset of Figure 1b and S10). In all cases, AFM and TEM analysis showed that the growth of the PFS_{54}–PP_{290} block copolymer occurs competitively along all three orthogonal axes of the central cylindrical PFS_{34}–$P2VP_{272}$ seed (see Figure S13). For example, an AFM height image of the oval micelles (Figures 1c and S11, prepared using the conditions in entry 4 of Table S3,) confirmed the presence of the original cylinder seed initiator of PFS_{34}–$P2VP_{272}$ in the center of the micelle. According to the cross section height profiles, the top of the micelle is essentially planar (Figure 1c–e in green) except in the location of the central seed, which corresponds to the highest point (ca. 24 nm, Figure 1c, e in dark red). The width of the selected micelle was around 200 nm and the central seed had a diameter of approximately 30 nm. The larger value compared with that obtained for the cylindrical seed micelles (ca. 10 nm, Figure S6) supports a 3D growth mechanism for the PFS_{54}–PP_{290} around the central seed micelle, as implied in the proposed depiction of the structure in Figure 1f. Ovals are a rarely observed morphology in the field of block copolymer self-assembly. To our knowledge, this is the first time that pointed-oval-shaped micelles have been prepared as a single, reproducible morphology. The reports of their formation that do exist describe the preparation of oval nanostructures as a mixture with spherical micelles and with no uniform shape or size.[21]

To obtain pointed ovals with a more uniform size we used a shorter PFS_{34}–$P2VP_{272}$ cylindrical seed sample that was more monodisperse in length. These shorter cylinders were prepared by sonication of a cylindrical micelle solution of PFS_{34}–$P2VP_{272}$ (prepared as described above) in *i*PrOH (0.33 mg mL^{-1}) over 20 min at −78 °C.[15c] After this process, we obtained a solution of smaller seeds (with $L_n = 63$ nm versus 215 nm) and significantly narrower L_w/L_n value (1.31 versus 1.63) as determined by TEM (Figures S4b, S5b, and S7). We then took 50 μL of the seed solution and, after dilution with 2 mL of *i*PrOH, added sequentially, five times, 200 μL of a solution of PFS_{54}–PP_{290} in THF (10 mg mL^{-1}). Before each addition, the solution was aged 24 h and analyzed by dynamic light scattering (DLS) to confirm the absence of remaining unimers, and 1 mL of *i*PrOH was added to avoid dissolution of the micelles due to an increase in the mole fraction of THF present. The DLS analysis of the micellization process revealed that $R_{h,app}$ increased gradually from 32.5 nm (seed solution) to 250 nm after the fifth addition (Figure S9 and Table S5). TEM analysis 24 h after each addition of unimers revealed the gradual formation of pointed-oval-shaped micelles of PFS_{54}–PP_{290} around the seed.

The shape and the size control achieved by using better defined seeds were much improved. After the third addition, very uniform pointed-oval-shaped nanostructures with controlled size depending on the amount of unimers added were

obtained (Figure 2a,b and also S12). The TEM images also revealed the history of the growth process corresponding to the different additions as regions of different TEM contrast within the micelle (Figure 2b). Subsequent additions of unimers beyond the fifth addtion resulted in aggregation of the nanostructures and the formation of cloudy solutions.

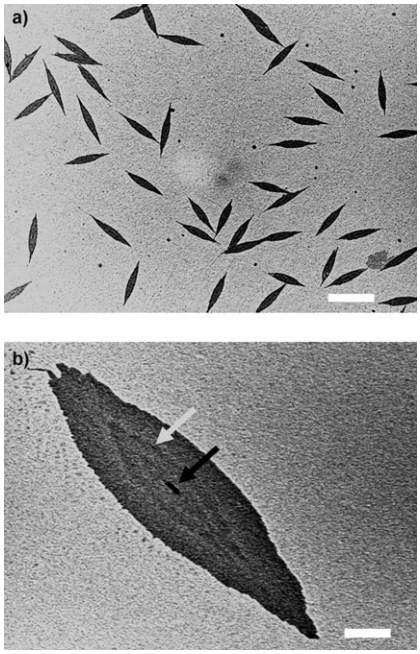

Figure 2. Bright field TEM images of the pointed-oval nanostructures obtained by sequential addition: a) After the fourth addition and b) after the fifth addition (see Figure S12 for bright field TEM images of the first three additions). The black and white arrows show the central seed, and evidence of the growth arising from previous additions, respectively. Scale bars correspond to 2000 nm (a) and 500 nm (b).

We have also explored the use of the pointed-oval-shaped micelles themselves as precursors to hierarchical micelle architectures through crystallization-driven living self-assembly. Specifically, we examined whether it would be possible to grow a cylindrical micelle brush epitaxially from the surfaces. We took 1 mL of the micelle solution (prepared by sequential addition of PFS_{54}–PP_{290} in THF to the PFS_{34}–$P2VP_{272}$ seed micelles in *i*PrOH) followed by dilution with 1 mL of *i*PrOH. To this solution we added 15 μL aliquots of PFS_{34}–$P2VP_{272}$ in THF (10 mg mL^{-1}). The $R_{h,app}$ value of the micelles increased gradually from 93 nm (pointed-oval-shaped micelles) and reached a constant value (145 nm) after 24 h. Clear evidence for an increase in micelle length was also revealed by TEM analysis (Figure S14) where elongation along the long axis of the micelles with the external growth of a cylinder was detected. In previous work, multiple cylinders were grown from selective faces of rectangular platelet crystals by a similar technique.[15b] We repeated the process three more times, adding 15 μL of PFS_{34}–$P2VP_{272}$ solution in THF (10 mg mL^{-1}) each time. We clearly observed elongation of the cylinders and the formation of multiple cylinders along the long axis of the pointed-oval-shaped micelles by TEM (Figure 3a).

It is important to note that neither free cylinders nor ovals without cylinders were found in any of the samples analyzed by TEM. This indicates that the epitaxial cylinder growth initiated by the micelles is very efficient and is much faster than the formation of free cylinders that would occur in the absence of a seed material. The epitaxially grown external cylinders had a diameter of (38 ± 2) nm, on the basis of AFM analysis (Figure 3b, S17, S18, and S19) as well as a core diameter of 12 nm (TEM analysis) and a modestly broad length distribution, with a number-average length L_n = 635 nm and weight-average length L_w = 952 nm (L_w/L_n = 1.48). Their height as established by AFM analysis was 13 nm (Figures S17 and S18). Importantly, AFM phase images (Figure S16) showed that the PFS_{34}–$P2VP_{272}$ grows epitaxially all around the pointed-oval shape, but preferentially along the long axis of the oval as cylinders.

In summary, we have successfully obtained pointed-oval-shaped micelles of uniform shape and size by crystallization-driven living self-assembly of PFS_{54}–PP_{290} diblock copolymer using seed initiators of PFS_{34}–$P2VP_{272}$ and a selective solvent (*i*PrOH) for the PP and P2VP blocks. Analysis of the AFM data clearly showed 3D growth of PFS_{54}–PP_{290} around the seed of PFS_{34}–$P2VP_{272}$ (compared to 1D or 2D growth that has been found in previous work).[15] This is achieved by the interplay of the relative rates of growth in all three orthogonal directions around the seed, creating well-defined micelles

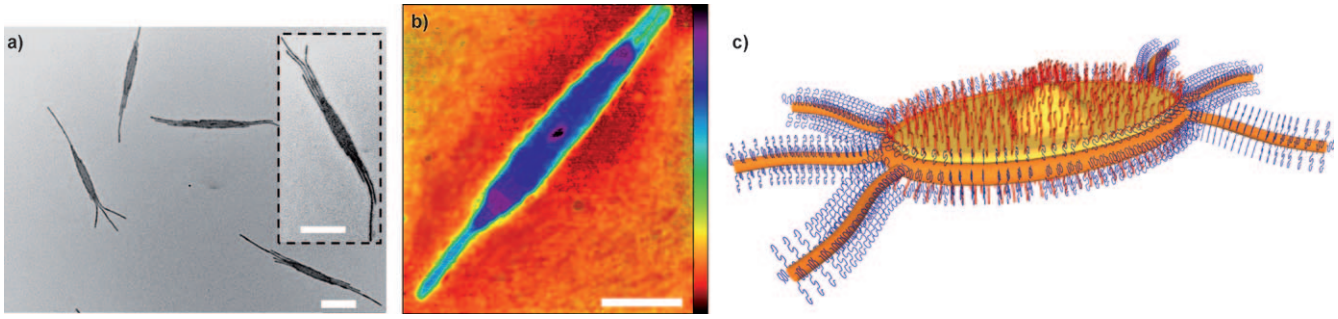

Figure 3. a) Bright field TEM images after the sequential additions of PFS_{34}–$P2VP_{272}$ to a micelle solution of PFS_{54}–PP_{290} (initiator) after the fourth addition (additional TEM images: Figures S14–S15). b) AFM height image of the micelle. c) Idealized graphic representation of the micelle. The PFS core is represented in orange (central cylinder, ribbon around the pointed oval and cylinder tassels growing outside the pointed oval, PFS–P2VP) and yellow (body of the pointed oval of PFS–PP), and the coronas in red (PP) and blue (P2VP). Scale bars correspond to 500 nm.

with curved shapes. These pointed-oval-shaped micelles can themselves be used as templates to grow hierarchical structures where cylindrical micelles of PFS_{34}–$P2VP_{272}$ are grown preferentially off of the ovals along the long axis. The ability to create well-defined curved shapes combined with the already demonstrated spatially defined decoration of self-assembled nanostructures with coatings such as titania, metal nanoparticles and quantum dots,[16] suggests that crystallization-driven living self-assembly offers many possibilities for the creation of tailored functional nanomaterials with significant applications.

Received: May 20, 2010
Published online: September 21, 2010

Keywords: block copolymers · living polymerization · metallopolymers · micelles · self-assembly

[1] a) I. W. Hamley, *Angew. Chem.* **2003**, *115*, 1730 – 1752; *Angew. Chem. Int. Ed.* **2003**, *42*, 1692 – 1712; b) D. E. Discher, A. Eisenberg, *Science* **2002**, *297*, 967 – 973; c) M. Lazzari, M. A. López-Quintela, *Adv. Mater.* **2003**, *15*, 1583 – 1594; d) J.-F. Gohy, *Adv. Polym. Sci.* **2005**, *190*, 65 – 136; e) Y. Kim, P. Dalhaimer, D. A. Christian, D. E. Discher, *Nanotechnology* **2005**, *16*, S484 – S491; f) L. Cao, J. A. Massey, M. A. Winnik, I. Manners, S. Riethmüller, F. Banhart, J. P. Spatz, M. Möller, *Adv. Funct. Mater.* **2003**, *13*, 271 – 276.

[2] a) N. S. Cameron, M. K. Corbierre, A. Eisenberg, *Can. J. Chem.* **1999**, *77*, 1311 – 1326; b) E. B. Zhulina, M. Adam, I. LaRue, S. S. Sheiko, M. Rubinstein, *Macromolecules* **2005**, *38*, 5330 – 5351; c) J. Qian, M. Zhang, I. Manners, M. A. Winnik, *Trends Biotechnol.* **2010**, *28*, 84 – 92; d) R. C. Hayward, D. J. Pochan, *Macromolecules* **2010**, *43*, 3577 – 3584.

[3] a) M. Antonietti, S. Heinz, M. Schmidt, C. Rosenauer, *Macromolecules* **1994**, *27*, 3276 – 3281; b) L. Zhang, A. Eisenberg, *Science* **1995**, *268*, 1728 – 1731; c) J. P. Spatz, S. Mößmer, M. Möller, *Angew. Chem.* **1996**, *108*, 1673 – 1676; *Angew. Chem. Int. Ed. Engl.* **1996**, *35*, 1510 – 1512; d) G. Liu, J. Ding, L. Qiao, A. Guo, B. P. Dymov, J. T. Gleeson, T. Hashimoto, K. Saijo, *Chem. Eur. J.* **1999**, *5*, 2740 – 2749; e) I. Korczagin, M. A. Hempenius, R. G. Fokkink, M. A. Cohen Stuart, M. Al-Hussein, P. H. H. Bomans, P. M. Frederik, G. J. Vancso, *Macromolecules* **2006**, *39*, 2306 – 2315.

[4] a) J. A. Massey, K. Temple, L. Cao, Y. Rharbi, J. Raez, M. A. Winnik, I. Manners, *J. Am. Chem. Soc.* **2000**, *122*, 11577 – 11584; b) L. Cao, I. Manners, M. A. Winnik, *Macromolecules* **2002**, *35*, 8258 – 8260; c) F. Wurm, S. Hilf, H. Frey, *Chem. Eur. J.* **2009**, *15*, 9068 – 9077.

[5] a) S. Jain, F. S. Bates, *Science* **2003**, *300*, 460 – 464; b) S. Jain, F. S. Bates, *Macromolecules* **2004**, *37*, 1511 – 1523.

[6] a) Z. Li, Z. Chen, H. Cui, K. Hales, K. Qi, K. L. Wooley, D. J. Pochan, *Langmuir* **2005**, *21*, 7533 – 7539; b) T. W. Schleuss, R. Abbel, M. Gross, D. Schollmeyer, H. Frey, M. Maskos, R. Berger, A. F. M. Kilbinger, *Angew. Chem.* **2006**, *118*, 3036 – 3042; *Angew. Chem. Int. Ed.* **2006**, *45*, 2969 – 2975.

[7] a) J. J. L. M. Cornelissen, M. Fischer, N. A. J. M. Sommerdijk, R. J. M. Nolte, *Science* **1998**, *280*, 1427 – 1430; b) J. Dupont, G. Liu, K.-I. Niihara, R. Kimoto, H. Jinnai, *Angew. Chem.* **2009**, *121*, 6260 – 6263; *Angew. Chem. Int. Ed.* **2009**, *48*, 6144 – 6147.

[8] a) A. Walther, M. Drechsler, S. Rosenfeldt, L. Harnau, M. Ballauff, V. Abetz, A. H. E. Müller, *J. Am. Chem. Soc.* **2009**, *131*, 4720 – 4728; b) I. K. Voets, A. de Keizer, P. deWaard, P. M. Frederik, P. H. H. Bomans, H. Schmalz, A. Walther, S. M. King, F. A. M. Leermakers, M. A. Cohen Stuart, *Angew. Chem.* **2006**, *118*, 6825 – 6828; *Angew. Chem. Int. Ed.* **2006**, *45*, 6673 – 6676.

[9] D. J. Pochan, Z. Chen, H. Cui, K. Hales, K. Qi, K. L. Wooley, *Science* **2004**, *306*, 94 – 97.

[10] a) K. Yu, L. Zhang, A. Eisenberg, *Langmuir* **1996**, *12*, 5980 – 5984; b) S. Stewart, G. Liu, *Angew. Chem.* **2000**, *112*, 348 – 352; *Angew. Chem. Int. Ed.* **2000**, *39*, 340 – 344.

[11] a) Z. Li, E. Kesselman, Y. Talmon, M. A. Hillmyer, T. P. Lodge, *Science* **2004**, *306*, 98 – 101; b) S. Kubowicz, J.-F. Baussard, J.-F. Lutz, A. F. Thünemann, H. von Berlepsch, A. Laschewsky, *Angew. Chem.* **2005**, *117*, 5397 – 5400; *Angew. Chem. Int. Ed.* **2005**, *44*, 5262 – 5265.

[12] a) L. Zhang, C. Bartels, Y. Yu, H. Shen, A. Eisenberg, *Phys. Rev. Lett.* **1997**, *79*, 5034 – 5037; b) I. C. Riegel, A. Eisenberg, C. L. Petzhold, D. Samios, *Langmuir* **2002**, *18*, 3358 – 3363.

[13] J.-K. Kim, M.-K. Hong, J.-H. Ahn, M. Lee, *Angew. Chem.* **2005**, *117*, 332 – 336; *Angew. Chem. Int. Ed.* **2005**, *44*, 328 – 332.

[14] For work on the solution self-assembly of organic crystalline-coil block copolymers see: a) T. Vilgis, A. Halperin, *Macromolecules* **1991**, *24*, 2090 – 2095; b) J. Fu, B. Luan, X. Yu, Y. Cong, J. Li, C. Pan, Y. Han, Y. Yang, B. Li, *Macromolecules* **2004**, *37*, 976 – 986; c) J. Zhang, L.-Q. Wang, H. Wang, K. Tu, *Biomacromolecules* **2006**, *7*, 2492 – 2500; d) M. Lazzari, D. Scalarone, C. E. Hoppe, C. Vazquez-Vazquez, M. A. Lopez-Quintela, *Chem. Mater.* **2007**, *19*, 5818 – 5820; e) Z.-X. Du, J.-T. Xu, Z.-Q. Fan, *Macromolecules* **2007**, *40*, 7633 – 7637; f) D. Portinha, F. Boue, L. Bouteiller, G. Carrot, C. Chassenieux, S. Pensec, G. Reiter, *Macromolecules* **2007**, *40*, 4037 – 4042; g) Z.-X. Du, J.-T. Xu, Z.-Q. Fan, *Macromol. Rapid Commun.* **2008**, *29*, 467 – 471; h) M. Lazzari, D. Scalarone, C. Vazquez-Vazquez, M. A. López-Quintela, *Macromol. Rapid Commun.* **2008**, *29*, 352 – 357; i) H. Schmalz, J. Schmelz, M. Drechsler, J. Yuan, A. Walther, K. Schweimer, A. M. Mihut, *Macromolecules* **2008**, *41*, 3235 – 3242; j) A. M. Mihut, M. Drechsler, M. Möller, M. Ballauff, *Macromol. Rapid Commun.* **2010**, *31*, 449 – 453.

[15] a) X. Wang, G. Guerin, H. Wang, Y. Wang, I. Manners, M. A. Winnik, *Science* **2007**, *317*, 644 – 647; b) T. Gädt, N. S. Ieong, G. Cambridge, M. A. Winnik, I. Manners, *Nat. Mater.* **2009**, *8*, 144 – 150; c) J. B. Gilroy, T. Gädt, G. R. Whittell, L. Chabanne, J. M. Mitchels, R. M. Richardson, M. A. Winnik, I. Manners, *Nat. Chem.* **2010**, *2*, 566 – 570.

[16] a) H. Wang, W. Lin, K. P. Fritz, G. D. Scholes, M. A. Winnik, I. Manners, *J. Am. Chem. Soc.* **2007**, *129*, 12924 – 12925; b) H. Wang, A. J. Patil, K. Liu, S. Petrov, S. Mann, M. A. Winnik, I. Manners, *Adv. Mater.* **2009**, *21*, 1805 – 1808.

[17] H. Wang, M. A. Winnik, I. Manners, *Macromolecules* **2007**, *40*, 3784 – 3789.

[18] a) A. P. Soto, I. Manners, *Macromolecules* **2009**, *42*, 40 – 42; b) H. R. Allcock, S. D. Reeves, J. M. Nelson, C. A. Crane, I. Manners, *Macromolecules* **1997**, *30*, 2213 – 2215.

[19] For full experimental details see the Supporting Information.

[20] Preliminary studies showed that solution self-assembly of PFS_{54}–PP_{290} in *i*PrOH (selective for the PP block) gave a mixture of spheres and platelets whereas in MeOH only spheres were formed (Figure S1).

[21] See, for example: a) P. Dimitrov, A. Porjazoska, C. P. Novakov, M. Cvetkovska, C. B. Tsvetanov, *Polymer* **2005**, *46*, 6820 – 6828; b) T. Arai, J. Ogawa, E. Mouri, M. P. I. Bhuiyan, N. Nishino, *Macromolecules* **2006**, *39*, 1607 – 1613.

